Available online at www.sciencedirect.com
SCIENCE DIRECT®
Journal of Solid State Chemistry 177 (2004) 844–848
JOURNAL OF SOLID STATE CHEMISTRY
http://elsevier.com/locate/jssc

Synthesis of novel mesoporous silica spheres with starburst pore canal structure

Yan-Bo Zhang, Xue-Feng Qian,* Zhong-Kai Li, Jie Yin, and Zi-Kang Zhu

School of Chemistry and Chemical Technology, Technology Research Institute of Polymer Materials, State Key Laboratory of Composite Materials, Shanghai Jiao Tong University, Shanghai 200240, PR China

Received 27 May 2003; received in revised form 26 August 2003; accepted 24 September 2003

Abstract

Novel spherical mesoporous silica materials with uniform diameters and starburst mesopore structures were synthesized by a simple one-step procedure with ethanol as the co-solvent in dilute aqueous solution and their formation mechanism was proposed. The arrangement of the pore canal and the diameter of the sphere could be tailored by altering the concentration of ethanol.

Keywords: Mesoporous materials; Starburst pore canal; Mesoporous silica sphere

1. Introduction

Mesoporous materials such as M41S have attracted much attention due to their important role in fields such as adsorption, catalysis and separation. Generally, mesoporous silica could be synthesized by the acid route [1] or the alkaline route [2]. Recently some successes have been achieved to synthesize mesoporous silica with different morphologies and particle diameters in dilute alkaline solution, which will open up possibilities for applications in special fields of chromatography and catalysis due to easy handling and packing [3]. As a rule, mesoporous silica with spherical shape could be obtained by simply adjusting the molar ratio between the silicate and cationic surfactant in proper alkaline solutions due to the mechanism of self-assembly of micelles. For example, Cai et al. [3] and Ostafin et al. [4] synthesized nanoscale mesoporous silica spheres with controlled particle size in aqueous solution. Recently, studies found that the addition of organic solvents such as alcohols [5] and toluene [6] had great effects on the particle morphology and the structure of mesporous silica prepared in alkaline solution. In the preparation process, these organic solvents act not only as the co-solvent leading to the formation of more spherical spheres but also as the co-surfactant to balance the hydrophilic and hydrophobic groups leading to the formation of novel mesopore structures. For example, Schumacher et al. [7] prepared mesoporous material MCM-48 with an ordered mesopore structure and more spherical morphology with ethanol as the co-solvent. Mou et al. synthesized tubule-within-tubule [8] and pillar-within-sphere [9] novel forms of MCM-41 in different media of alcohols.

In this work, novel mesoporous silica spheres were prepared. They have uniform diameter and their mesopore canals are starburst (emanating from the center to the exterior surface), which is quite different from the mesoporous materials reported in previous articles. The novel mesoporous silica spheres can be obtained by simply adjusting the concentration of water and ethanol in alkaline medium. The effects of ethanol on the micelle structure and morphology transformation are discussed, and the formation mechanism is proposed.

2. Experimental section

In a typical process, cetyltrimethyl ammonium bromide (CTAB) was dissolved in the mixture of sodium hydroxide aqueous solution and ethanol with vigorous stirring at corresponding temperatures and molar ratios according to Table 1. After 30 min, tetraethoxysilane

*Corresponding author. Fax: +86-21-54741297.
E-mail address: xfqian@sjtu.edu.cn (X.-F. Qian).

0022-4596/$ - see front matter © 2003 Elsevier Inc. All rights reserved.
doi:10.1016/j.jssc.2003.09.018

Table 1
Synthesis conditions and morphology of samples

Sample	Composition/mol ratio H_2O:CTAB:TEOS:NaOH:EtOH	T/K	Morphology of sample
A	2486:0.123:1:0.63:0	353	Irregular spheres with ordered hexagonal mesopore canal
B	2330:0.123:1:0.63:46.5	353	Spheres including egg-like shell and amorphous lamella
C	2133:0.123:1:0.63:109	353	Heterogeneous spheres with starburst mesopore canal
D	1984:0.123:1:0.63:155	353	Homogeneous spheres with starburst mesopore canal
E	1736:0.123:1:0.63:233	353	Particles without mesopore structure

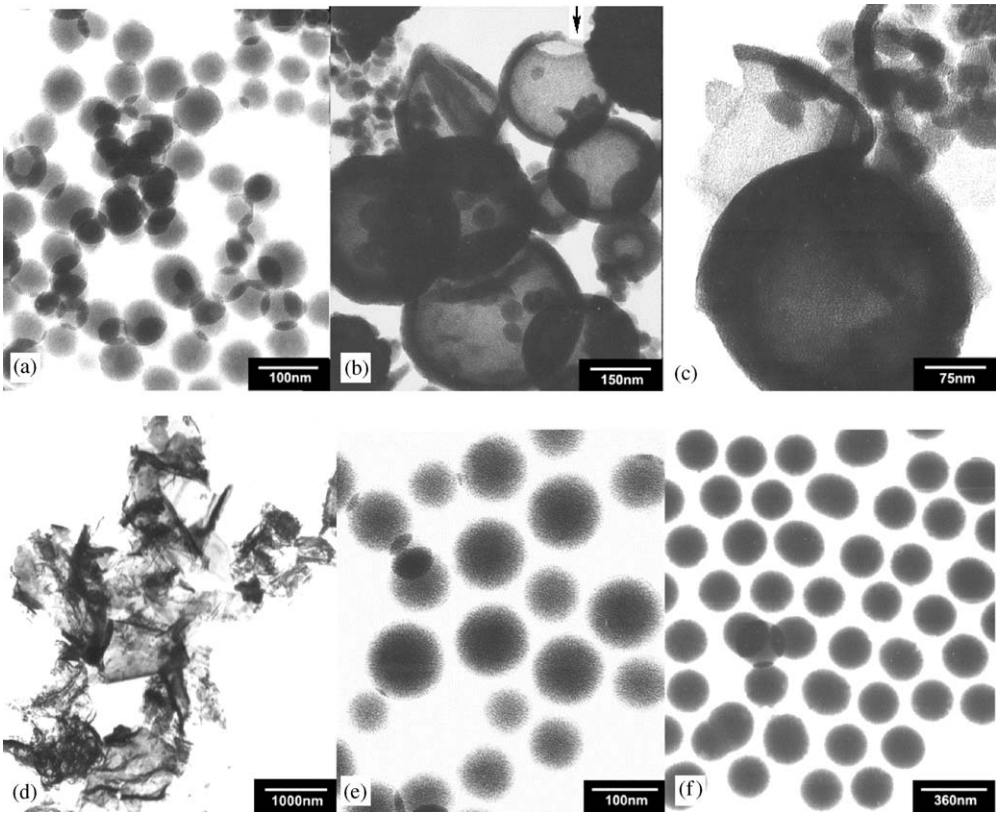

Fig. 1. TEM images of the mesoporous silica spheres showing (a) sample A; (b) general and (c) close views of sample B; (d) lamellar phase in sample B; (e) sample C and (f) sample D.

(TEOS) was added to the suspension and the reaction was carried out for another 3 h. The compound was transferred to a beaker to precipitate for 24 h, then was filtered and washed consecutively with ethanol and distilled water several times. The as-synthesized samples were calcined at 823 K for 5 h in air after being aged at ambient temperature.

3. Results and discussion

From Table 1, samples A to E were synthesized in weak alkaline solutions of CTAB and TEOS. The morphology of sample A, shown in Fig. 1(a), is in near spherical shape with diameters less than 100 nm over a narrow range. The pores, were found to be ordered and regular, align over long range in nanoparticles which is consistent with the XRD pattern of Fig. 3(a). The observation of typical diffraction peaks between $2\theta = 2^\circ$ and 5° indicates the presence of an ordered hexagonal array of parallel silica tubes and can be indexed assuming a hexagonal unit cell as (100), (110), (200), and (210) of MCM-41 [10]. The formation mechanism of mesoporous silica MCM-41 is shown in pathway I of Scheme 1, which includes the steps of (1) hydrolysis of TEOS and (2) self-organization of surfactant, and then combination of surfactant and silicate oligomers. The pathway I is the liquid-crystal-initiated templating (LCIT) mechanism proposed by Beck et al. [11] which represented the hexagonal array of the micellar rods.

Samples B–D were synthesized with a gradually increased quantity of ethanol according to Table 1. It

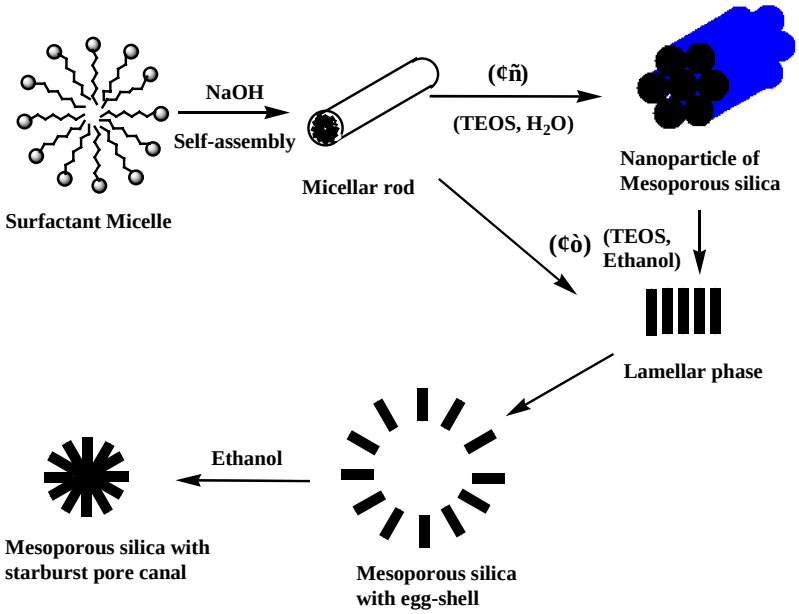

Scheme 1. Possible mechanistic pathways for the formation of meso-silica materials with nanospheres, eggshell and starburst pore canals.

is interesting to find that spheres with eggshells were obtained in sample B though some spherical nanoparticles could still be found in the TEM image of Fig. 1(b). The close view of sample B is shown in Fig. 1(c). The pore canals are perpendicular to the eggshell of the ring-shaped spheres and the array of mesopores in the nanospheres is still ordered. A half eggshell in Fig. 1(c) and a gap pointed in Fig. 1(b) are both proof of the formation of an eggshell, which indicates that the addition of ethanol changed the array of micelles. In the preparation process, some flakes which is shown in Fig. 1(d) were found of sample B in early stage, which indicates the formation of the lamellar phase of micelles in the system. The possible formation route is proposed in pathway II of scheme 1. Firstly, micelles of surfactant and micellar rods are formed in very dilute aqueous solution which is the same as pathway I. Secondly, the rods self-assemble to the lamellar phase or the hexagonal array transforms to the lamellar phase by the effect of ethanol because ethanol, as a polar solvent, plays a role in decreasing the aggregation and/or aggregate size of CTAB, and leads to the formation of a highly disordered packed phase when the concentration of CTAB is low [12]. The similar observation was also presented in the work of Mou et al. They assumed that mixed lamellar-hexagonal membrane formed and separated by the water layers in the surfactant-silicate system, then the lamellas curl to form capsules which later grow more compact and smaller [13]. The reasons may be that (1) the elastic energy of a homogeneously curved surface is small [13], and (2) a great amount of ethanol in the aqueous solution inhibits the hydrolysis of TEOS [3].

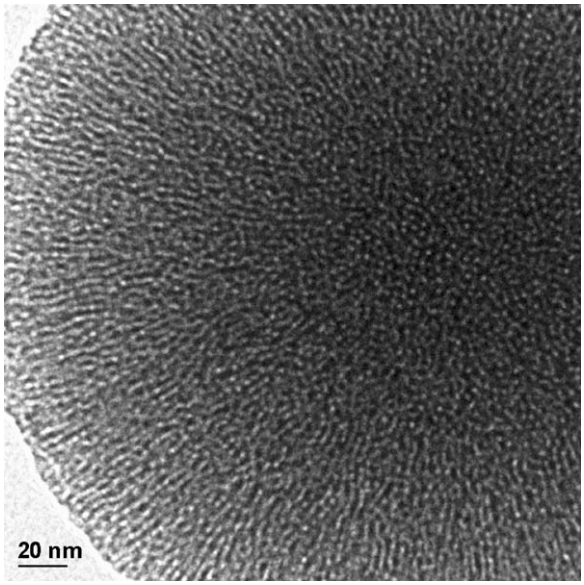

Fig. 2. HRTEM image showing sample D.

With further increase of ethanol, sample C (TEM image is shown in Fig. 1(e)) are all in spherical shape with a diameter of less than 100 nm and with the starburst pore canals radiating from the center to the surface of the sphere. Fig. 1(f) and Fig. 2 are the general view and HRTEM image of sample D, respectively. Fig. 1(f) shows well-dispersed spheres with uniform diameter of about 250 nm and Fig. 2 clearly shows that the mesopore canals radiate from the center to the circumference. The curves of $b-d$ of Fig. 3 correspond to the XRD patterns of samples B–D. From the data of the inset of Fig. 3, the repeat distance a_0 decreases from samples A to D, which indicates that the rod array is

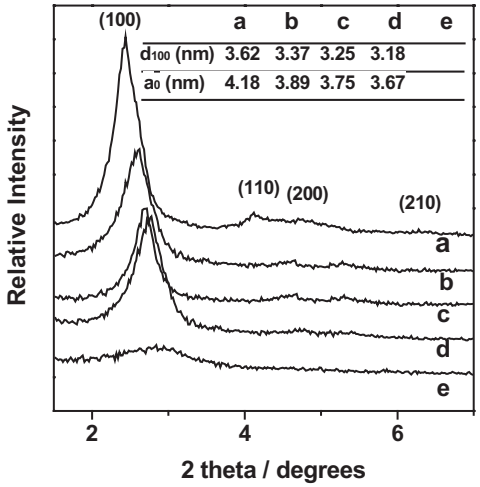

Fig. 3. XRD diffraction patterns of (a) sample A; (b) sample B; (c) sample C; (d) sample D; and (e) sample E. The inset shows the values of d_{100} and a_0 (the repeat distance) of samples.

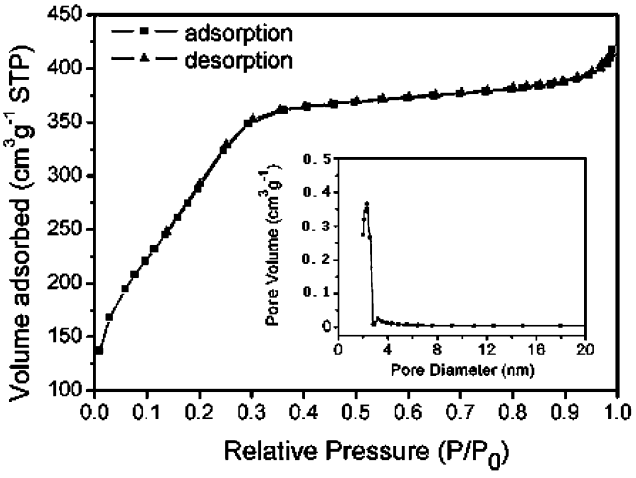

Fig. 4. Nitrogen adsorption–desorption isotherm (main plot) and pore size distribution curve (inset) of the calcined sample D.

more compact under the effect of ethanol in contrast to the medium of water.

Although it is known that a highly condensed and compact structure tends to be formed in alkaline medium because alkaline catalysis favors both hydrolysis and condensation of silicate [14], the mechanism of the effect of ethanol on the formation of more compact and uniform spheres in the last step of Scheme 1 is not completely clear. The role of ethanol in micelle arrangement is also found in sample E. With increasing ethanol amount, no diffraction peaks were found in curve *e* of Fig. 3, which indicates that no ordered structure could be obtained because the existence of a large amount of ethanol destroys the balance between the silicate condensation and silica reprecipitation which in succession destroys the formation of the mesoporous phase.

Fig. 4 shows the nitrogen adsorption–desorption isotherm (main plot) and the pore size distribution curve (inset figure) of the calcined sample D. The nitrogen adsorption isotherm of sample D is typically Type IV in the IUPAC classification of mesoporous materials. When the relative pressure (P/P_0) is very low (0–0.27), the leap in the curve can be due to the capillary condensation of nitrogen in the channels of the mesopores [15]. However, the absence of a hysteresis loop between the curves of the adsorption and desorption of nitrogen indicates that the adsorption is a monolayer of N_2 on the wall of the pores and no condensation has taken place in the pores or the phases between the particles. The data calculated from the curves indicate that the sample has relatively high specific surface area and total pore volume with a primary pore size of 2.65 nm, a specific surface area 1100 m^2/g and a total pore volume 0.647 cm^3/g. Generally, the nitrogen adsorption–desorption isotherm of mesoporous silica prepared with hydro-thermal methods has a hysteresis loop due to the existence of irregular flakes in the samples and the condensation of nitrogen in the gap channels between the flakes [16]. Therefore, the absence of a hysteresis loop further indicates that sample D prepared with the ethanol as the co-solvent has regular particles. Table 2 is the nitrogen adsorption–desorption isotherm data of samples A–D. It can be found that the adsorption average pore diameter reduced from samples A–D which is correspondence with the results of TEM studies, and BET surface area and pore volume also reduced.

Table 2
Nitrogen adsorption–desorption isotherm data of samples

Sample	BET surface area (m^2/g)	Specific pore volume (cm^3/g)	Adsorption average pore diameter (nm)
A	1260	1.20	3.97
B	1236	1.11	3.68
C	1163	0.86	3.24
D	1100	0.647	2.65

Fig. 5 shows the nitrogen adsorption-desorption isotherm (main plot) and the pore size distribution curve (inset figure) of the calcined sample A (MCM-41). The nitrogen adsorption isotherm of MCM-41 is also typically Type IV in the IUPAC classification of mesoporous materials. In contrast to the nitrogen adsorption–desorption isotherm of sample D (Fig. 3), the total adsorption of sample A falls at 400–500 cm^3/g, sample D 300–400 cm^3/g. It may be due to the novel structure of sample D, which easily leads to the mesopore filling in the relatively low pressure.

In the preparation process, ethanol, as a co-solvent, on the one hand disrupts the self-assembly of surfactant micelles due to the prevention of the hydrolysis of

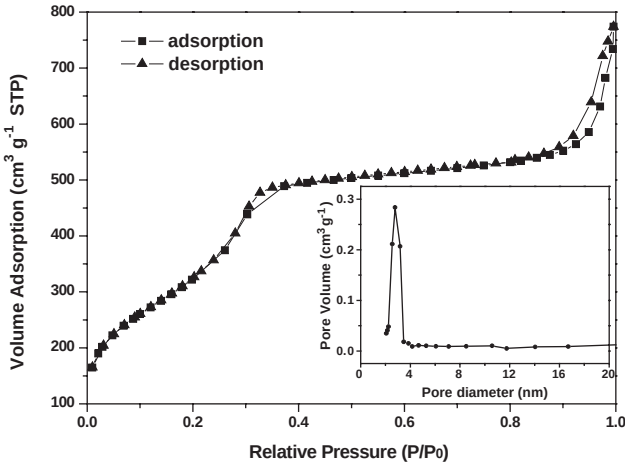

Fig. 5. Nitrogen adsorption–desorption isotherm (main plot) and pore size distribution curve (inset) of the calcined sample A.

silicate or the decrease of the surfactant aggregate for the weak solvophobic effect [17]. On the other hand, ethanol may act as a 'spacing agent' to adjust the interaction between ethanol and the cationic surfactant and the hydrophilic–hydrophobic balance of the self-assembly system [18]. Therefore, ethanol is also a co-surfactant.

4. Conclusions

Both the mesopore phase structure and morphology of mesoporous silica could be easily tailored with the addition of ethanol in the alkaline synthesis system. The samples synthesized in our work are novel mesoporous materials not belonging to any family of mesoporous materials reported previously. These novel mesoporous materials are believed to have further applications such as capsules of reaction and catalysts owing to the novel microscopically starburst structure of mesopore with macroscopically regular spherical shape. The addition of ethanol would help to extend the catalytic activities and opto-electronic properties of further embedded materials such as metal [7] or semiconductor [19] doped mesoporous materials because ethanol is a proper solvent for many precursors of metal and their oxides. Currently, the influence of ethanol concentration on microscopic structure of materials is being studied and further experiments are underway to prepare novel mesoporous materials with other co-solvents.

Acknowledgments

This work was financially supported by the National Natural Foundation of China (50103006), the Shanghai ShuGuang Project and the Shanghai Nanomaterials Project (0241nm106).

References

[1] Q. Huo, D.I. Margolese, U. Clesla, P. Feng, T.E. Gler, P. Sieger, R. Leon, P.M. Petroff, F. Schuth, G.D. Stucky, Nature 368 (1994) 317–321.
[2] C.T. Kresge, M.E. Leonowicz, W.J. Roth, J.C. Vartuli, J.S. Beck, Nature 359 (1992) 710–712.
[3] Q. Cai, Z.S. Luo, W.Q. Pang, Y.W. Fan, X.H. Chen, F.Z. Cui, Chem. Mater. 13 (2001) 258–263.
[4] R.I. Nooney, D. Thirunavukkarasu, Y. Chen, R. Josephs, A.E. Ostafin, Chem. Mater. 14 (2002) 4721–4728.
[5] M. Etienne, B. Lebeau, A. Walcarius, New J. Chem. 26 (2002) 384–386.
[6] A. Lind, B. Spliethoff, M. Linden, Chem. Mater. 15 (2003) 813–818.
[7] K. Schumacher, M. Grun, K.K. Unger, Microporous Mesoporous Mater. 27 (1999) 201–206.
[8] H.P. Lin, C.Y. Mou, Science 273 (1996) 765.
[9] H.P. Lin, Y.R. Cheng, C.Y. Mou, Chem. Mater. 10 (1998) 3772–3776.
[10] U. Ciesla, F. Schuth, Microporous Mesoporous Mater. 27 (1999) 131–149.
[11] J.S. Beck, J.C. Vartuli, W.J. Roth, M.E. Leonowicz, C.T. Kresge, K.D. Schmitt, C.T.W. Chu, D.H. Olson, E.W. Sheppard, S.B. McCullen, J.B. Higgins, J.L. Schlenker, J. Am. Chem. Soc. 114 (1992) 10834–10843.
[12] M.T. Anderson, J.E. Martin, J.G. Odinek, P.P. Newcomer, Chem. Mater. 10 (1998) 311–321.
[13] H.P. Lin, Y.R. Cheng, C.Y. Mou, Chem. Mater. 10 (1998) 3772–3776.
[14] C.Y. Mou, H.P. Lin, Pure Appl. Chem. 72 (2000) 137–146.
[15] P.I. Ravikovitch, D. Wei, W.T. Chueh, G.L. Haller, A.V. Neimark, J. Phys. Chem. B 101 (1997) 3671–3679.
[16] R. Leon, D. Margolese, G.D. Stucky, P.M. Petroff, Phys. Rev. B 52 (1995) 2285–2288.
[17] H.P. Lin, C.P. Kao, C.Y. Mou, Microporous Mesoporous Mater. 48 (2001) 135–141.
[18] H.P. Lin, Y.R.C.S.B. Liu, C.Y. Mou, J. Mater. Chem. 9 (1999) 1197–1201.
[19] D.O. Chomski, A. Kuperman, N. Coombs, G.A. Ozin, Chem. Vap. Deposit. 2 (1) (1996) 8–13.